Tunneling study of surface quantization in n-PbTe

D. C. Tsui, G. Kaminsky, and P. H. Schmidt
Bell Laboratories, Murray Hill, New Jersey 07974
(Received 27 November 1973)

Using electron tunneling through n-type PbTe-oxide-Pb junctions, we have measured some electronic properties of the (100) surface accumulation layer at the PbTe-oxide interface. Three energy levels, resulting from quantization of the electronic motion normal to the surface, are observed in a sample having $n=1.2\times10^{18}/\mathrm{cm}^2$. The energies of these three levels are $E_0=42$ meV, $E_1=19$ meV, and $E_2=6$ meV below the conduction band edge. From the magnetotunneling data we obtain $g^*=29\pm3$ and $m^*=(0.069\pm0.008)m_0$ for the ground-state subband. In addition, the Landau levels in the ground-state subband do not cross the Landau levels in the excited-state subband. The interaction between the Landau levels removes the degeneracy at the crossover and a splitting, $\Delta E\approx4$ meV, has been observed.

I. INTRODUCTION

Recently, the tunneling technique has been applied to the study of electronic surface states resulting from quantization of space-charge layers at semiconductor surfaces.[1,2] This technique measures directly the energy levels of the surface states and is most suited for studying the accumulation layers of degenerate bulk materials[3,4] on which conventional surface transport measurements are difficult. We describe a tunneling experiment on the (100) surface of degenerate n-type PbTe, using PbTe-oxide-Pb junctions, and we discuss the results pertinent to the quantization of the PbTe accumulation layer at the PbTe-oxide interface. These results constitute the first direct evidence for the long-anticipated surface-quantization effects in PbTe.[5]

The energy diagram of an idealized n-type PbTe-oxide-Pb tunnel junction, with an electron accumulation layer at the PbTe-oxide interface, is shown in Fig. 1. The energies E_n (with $n=0$, 1 and 2) indicate the quantum levels supported by the one-dimensional potential well $U(z)$ associated with the accumulation layer. Corresponding to each quantum level E_n, there is a band of two-dimensional conducting states whose band minimum is E_n. These two-dimensional energy bands are called the electric subbands.[6] Electrons in these subbands as well as those in the conduction band can contribute to tunneling through the oxide barrier. Ben-Daniel and Duke[3] have shown that when a bias voltage V is applied to the junction, the tunnel conductance (dI/dV) due to the subband electrons is directly proportional to the density of states η_s of the subband at an energy eV away from the Fermi level (μ) of the sample, i.e.,

$$dI/dV\propto\eta_s(\mu-eV) \quad . \tag{1}$$

Since η_s of a two-dimensional energy band has a step function discontinuity at the band edge, we expect a sudden decrease in conductance in the $dI/dV-V$ curve and, therefore, a dip in the d^2I/dV^2-V curve when eV is equal to the energy of a quantum level, as measured from μ. When a magnetic field H is applied perpendicular to the plane of the junction, it quantizes each two-dimensional subband into discrete spin-split Landau levels and splits the density of states into a series of δ-function peaks at the energy of the spin-split Landau levels. However, because of level broadening, we expect these peaks to be rounded off and appear as oscillations in the dI/dV-V and the d^2I/dV^2-V curves.

In this experiment, we have observed the surface quantum levels in the normal-state tunneling

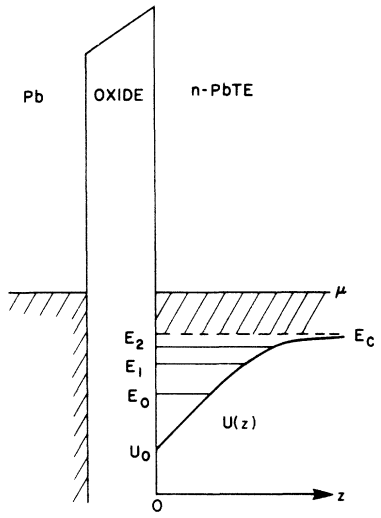

FIG. 1. An energy diagram for n-type PbTe-oxide-Pb tunnel junction with an electron accumulation layer at the PbTe-oxide interface. E_0, E_1, and E_2 indicate the quantum energy levels supported by the one-dimensional potential well $U(z)$ of the accumulation layer. U_0 is the depth of the well at the interface $z=0$.

data and the spin-split Landau levels of the ground-state subband in the magnetotunneling data. These data are discussed in Sec. IV. Sections II and III describe the experimental details and the theoretical background, respectively. Section V gives a summary of this paper.

II. EXPERIMENTAL DETAILS

The tunnel junctions are fabricated on single-crystal PbTe platelets, approximately $8\times5\times0.5$ mm. These platelets are cut from a vapor-grown crystal by the use of an abrasive wire saw. The conventional spark-erosion method, which has been successfully used in cutting single-crystals metals of high perfection, was found to cause more damage to the samples. The electron concentration of these samples, determined by Hall measurements on the platelets at 4.2 °K, is $n=(1.2\pm0.2)\times10^{18}/\text{cm}^3$. The sample surface, which is parallel to within 1° of a crystallographic (100) plane, is prepared by first mechanically polishing it to an optical finish and then electropolishing it to remove any mechanical damage. The electrolyte used for the polishing is a solution of 20 g of potassium hydroxide, 45-ml water, 35-ml glycerol, and 20-ml ethyl alcohol. We use a platinum cathode and a current density of approximately 3 A/cm^2. The oxide is thermally grown on the surface by leaving the sample in an oxygen atmosphere at 68 °C for 3 h.

The oxidized surface is then insulated by collodion except for a narrow strip in the middle. The junctions are formed by evaporating cross strips of Pb about 2000-Å thick on the sample in a vacuum of 1×10^{-6} Torr. The area of the resulting junctions varies from 5×10^{-4} to 50×10^{-4} cm^2. We use indium metal to solder gold-wire leads to the Pb film and to the PbTe sample. The standard cross-strip configuration[7] is used to facilitate four-terminal measurements. The methods for obtaining dI/dV and d^2I/dV^2 data as a function of V and H have been described previously[1,8] and will not be repeated here.

We utilize the tunneling characteristics of superconducting Pb to check if electron tunneling is indeed the dominant current-carrying mechanism through the junction and follow the standard procedure for evaluating superconducting tunnel junctions.[8] It turns out that only about 10% of all the junctions which we have investigated show the proper tunneling characteristics of superconducting Pb at liquid-helium temperatures. We estimate from the I-V characteristic of these junctions at 1 °K that approximately 1% of the junction current arises from some nontunneling mechanisms. The normal-state resistance of most of these junctions changes by less than 20% as the temperature is changed from 300 to 4.2 °K. We regard this weak temperature dependence as an indication that the tunnel barrier is indeed an oxide barrier of height $\gtrsim1$ eV. It should be emphasized that the surface-quantization effects, discussed in this paper, have been observed only in these selected tunnel junctions.

III. THEORETICAL BACKGROUND

Before discussing the tunneling data, we need to recall some of the electronic properties of PbTe.[9] It has the NaCl crystal structure and its conduction band has multiple minima at the L symmetry points of the Brillouin zone of the fcc lattice. Because of the small direct energy gap at L ($E_g=0.19$ eV at 4.2 °K), the conduction band is highly nonparabolic. Extrinsic carriers are generated by deviations from stoichiometry and no freeze-out of these carriers has been detected at any temperature. The electron Fermi surface consists of four ellipsoids of revolution with their major axes oriented along the $\langle111\rangle$ directions. The transverse mass (m_t) and the longitudinal mass (m_l) at the band edge are $m_t=0.024m_0$ and $m_l=0.24m_0$. The anisotropic g values[10] are characterized by $g_\parallel=57.5$ and $g_\perp=15$.

According to Stern and Howard,[6] the two-dimensional subbands resulting from quantization of the accumulation layer on a PbTe (100) surface likewise have multiple energy minima. These minima occur at the X symmetry points of the two-dimensional Brillouin zone of the square lattice.[11] The constant energy contour in the k plane is four ellipses with major axes along the bulk crystallographic $\langle110\rangle$ directions in the plane. Figure 2 shows the Brillouin zone for the PbTe (100) surface and the constant-energy ellipses of a subband. Each point on the constant-energy ellipses is doubly degenerate. If we neglect the nonparabolicity

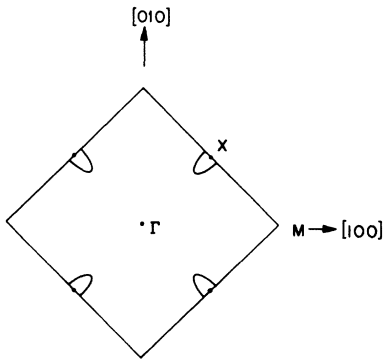

FIG. 2. Brillouin zone for the PbTe (100) surface and the constant-energy ellipses of a subband. Each point on the ellipses is doubly degenerate. $\Gamma M=2\pi/a$ and a is the lattice constant of PbTe.

of the conduction band, the subband near an energy minimum, corresponding to a quantum level E_n, is described by

$$E_n(k_1, k_2) = E_n + (\tfrac{1}{2}\hbar^2)(k_1^2/m_1 + k_2^2/m_2) \quad , \tag{2}$$

where m_1 and m_2 are the principal effective masses of the constant-energy ellipse, related to m_t and m_l of the bulk conduction band by

$$m_1 = m_t, \quad m_2 = \tfrac{1}{3}(m_t + 2m_l) \quad . \tag{3}$$

Stern and Howard also gave an approximate treatment of the Landau levels in a subband of a multivalley semiconductor, assuming no coupling between subbands. According to their results, when a magnetic field H is applied perpendicular to the (100) surface of PbTe, the energy levels of a subband, as measured from the zero-field band edge of the subband, are given by

$$E_l = (l + \tfrac{1}{2})\,[\hbar eH/(m_1 m_2)^{1/2}c] + f(H^2) \quad , \tag{4}$$

where the first term is the familiar harmonic-oscillator energy for the Landau levels and the second term is a correction, having a quadratic dependence on H and being independent of the Landau quantum number l. Thus, the cyclotron effective mass of electrons in the subband is

$$m^* = (m_1 m_2)^{1/2} \quad . \tag{5}$$

Using $m_t = 0.024m_0$, $m_l = 0.24m_0$ together with Eq. (3), we obtain $m^* = 0.063m_0$. It differs considerably from the bulk electron cyclotron mass ($0.038m_0$) when the magnetic field is oriented along [100]. This difference arises from the fact that electrons in the surface subbands, unlike those in the bulk, cannot have a velocity component parallel to the magnetic field.

Fang and Stiles[12] have observed the spin splitting in the magnetoconductance of electrons in a Si inversion layer. They demonstrated that the spin splitting in a subband is determined by the total magnetic field, not just the normal component. At present, however, there is still no theory treating Landau levels of the subbands including the electron spin and spin-orbit coupling.

IV. RESULTS AND DISCUSSION

A. Normal-state tunneling data

Figure 3 shows the dI/dV-V and the d^2I/dV^2-V curves of an n-type PbTe-oxide-Pb tunnel junction at 4.2 °K. As discussed in Sec. II, the junction is fabricated on a (100) surface of PbTe, whose electron concentration is $n = 1.2\times10^{18}/\text{cm}^3$. The superconductivity of the Pb electrode is quenched by an external magnetic field $H = 2.5$ kG. The weak structure near zero bias (at $|V| < 20$ mV) has been observed previously[13-15] and it is due to emission and self-energy effects of Pb phonons and PbTe phonons. The d^2I/dV^2 peaks at $V \approx 4.5$, 8.5, and 14.5 mV are identified as the TA and LA phonon peaks of Pb and the LO phonons of PbTe, respectively. The d^2I/dV^2-V curve also shows a step-like discontinuity at zero bias. This discontinuity has also been observed in the tunneling data from InAs-oxide-Pb[16] and Cr-oxide-Pb junctions.[17] There has not yet been any explanation for this anomalous structure.

As illustrated in the inset of Fig. 3, we have also resolved a weak structure in the d^2I/dV^2-V curves at $V \approx 36$ mV. This structure is due to the cutoff in the conduction-electron density of states at the PbTe conduction-band edge. Its bias position V_c is a direct measure of the Fermi energy μ of electrons in the conduction band of PbTe. By applying a magnetic field parallel to the sample surface, we have also observed oscillations in the d^2I/dV^2-H curves which reflect the Landau levels of the conduction band of PbTe. A parallel magnetic field cannot give rise to Landau levels in the subbands. Following a standard procedure,[1] we have determined $\mu = 36 \pm 2$ meV by extrapolating the observed Landau levels to $H = 0$. It agrees reasonably well with an estimated value of $\mu = 32$ meV, using $n = 1.2\times10^{18}/\text{cm}^3$, $m_t = 0.024m_0$, and $m_l = 0.24m_0$.

In the case of InAs reported earlier,[1,2] much stronger structure, reflecting the conduction-band edge of InAs, was observed in the dI/dV-V as well as the d^2I/dV^2-V data from InAs-oxide-Pb junctions. Zavadil[18] has explained this band-edge structure as due to the accumulation layer, which strongly enhances the tunneling probability of the conduction-band electrons near the band edge. This enhancement increases with increasing U_0, the

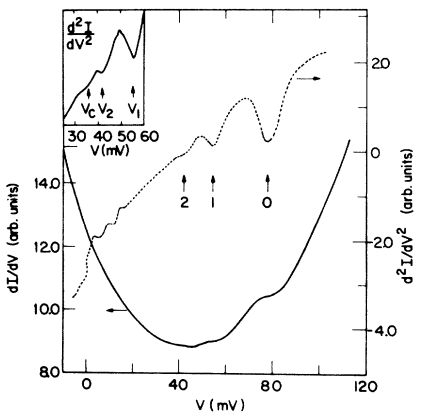

FIG. 3. dI/dV-V and d^2I/dV^2-V curves of an n-type PbTe-oxide-Pb junction at $T = 4.2$°K and $H \approx 2.5$ kG. The PbTe sample has $n = 1.2\times10^{18}/\text{cm}^3$.

depth of the surface potential well (Fig. 1). Although we do not measure U_0 directly in the tunneling experiments, it can be inferred from the experimentally measured binding energy of the quantum levels that U_0 is much smaller in the PbTe samples than in the InAs samples. Thus, Zavadil's explanation is also consistent with our observing a much weaker band-edge structure in PbTe.

The more prominent structure in Fig. 3 is the d^2I/dV^2 dips labeled as 0, 1, and 2 in the Pb (+) bias. These dips, corresponding to a sudden decrease in conductance at $V_0 = 78$ mV, $V_1 = 55$ mV, and $V_2 = 42$ mV, are due to the quantum energy levels in the potential well $U(z)$ of the PbTe surface accumulation layer (Fig. 1). We have examined the dI/dV-V and the d^2I/dV^2-V curves to $V = 100$ mV in the Pb (-) bias and to $V = 200$ mV in the Pb (+) bias and have not observed any additional structure. This fact enables us to conclude that there are three quantized levels in the surface potential well. The voltages V_0, V_1, and V_2, respectively, measure the energy of the ground state, the first excited state, and the second excited state, relative to the Fermi level of PbTe.

We should note that V_n measures the quantum level E_n when a bias equal to V_n is applied to the junction, i.e.,

$$eV_n = \mu + E_n(V_n) \quad . \tag{6}$$

Consequently, the structure of the quantum levels, observed in the tunneling data, is a true picture of that in the surface potential well without any external bias, only if the bias necessary for the observation has no appreciable effect on E_n. As discussed in the following paragraph, in our samples the applied bias has indeed no appreciable effect on E_n. Thus, the binding energy of the three quantum levels, using $\mu = 36$ meV, are $E_0 = 42$ meV, $E_1 = 19$ meV, and $E_2 = 6$ meV. If we approximate the lower portion of the surface potential well in PbTe (Fig. 1) by a triangular well and assume that E_0 and E_1 are correctly described by this triangular well,[19] the depth of the surface potential well is $U_0 = E_0 + (E_0 - E_1)/0.759 = 72$ meV.

The electron density in the surface accumulation layer can be estimated by counting the number of electrons in each subband, using

$$N_{sn} = n_v[(m_1 m_2)^{1/2}\pi\hbar^2]eV_n \quad . \tag{7}$$

Here, n_v is the number of constant-energy ellipses in a subband and, as seen in Fig. 2, is equal to 4. Using $m_1 = 0.024m_0$ and from Eq. (3) $m_2 = 0.168m_0$, we obtain $N_{s0} = 8.3\times10^{12}/\text{cm}^2$, $N_{s1} = 5.8\times10^{12}/\text{cm}^2$, and $N_{s2} = 4.5\times10^{12}/\text{cm}^2$ for the density in each subband. The total surface electron density is $N_s = 1.9\times10^{13}/\text{cm}^2$, and the electric field at the PbTe-oxide interface is $F_0 = 8\times10^4$ V/cm (using a static dielectric constant $\epsilon = 424$). We estimate from the junction capacitance that the bias necessary for observing the quantum levels can induce a surface charge density approximately two orders of magnitude smaller than N_s. Hence, it is reasonable to neglect the effect of this bias on E_n. In addition, we have not observed the magneto-oscillations in the d^2I/dV^2-V curves which are caused by the bias dependence of U_0.[1,4] This also suggests that the applied bias indeed has negligible effect on the surface accumulation layer.

Several aspects of the data deserve additional comments.

(i) The observed conductance decrease at V_n varies from approximately 8% at the ground-state level to approximately 1% at the second-excited-state level. This difference in the strength of the structure has been attributed to the increasing tunneling probability of electrons in the subbands with increasing applied bias.[1] Since the structure due to the ground-state level is observed at the largest bias, it is expected to be the strongest.

(ii) The width of the dip in the d^2I/dV^2-V curve at half its minimum depth is a direct measure of the level broadening of the quantum state. This half-width is approximately 10 mV (which gives a lifetime $\tau \approx 7\times10^{-14}$ sec) for the ground state and appears to be smaller for the excited states. This is understandable because the ground state is confined closest to the interface and is, therefore, most sensitive to surface irregularities.

(iii) The d^2I/dV^2 dip reflecting the ground-state quantum level has a shoulder on its large bias side. When the Pb electrode is in its superconducting state, this shoulder is resolved into a small dip at about $V = 86$ mV. We tentatively attribute it to a splitting of the ground-state level due to some local deviations of the surface from the (100) orientation.

(iv) We have obtained similar results from all the junctions which were proved to be tunnel junctions and whose normal-state resistance is approximately independent of temperature from $T = 300\,^\circ$K to $T = 1\,^\circ$K. The bias positions, at which the surface quantum levels are observed, varies by less than 10% among the different junctions on different samples, and the observed half-width of the d^2I/dV^2 dips varies by no more than 20%.

B. Magnetotunneling data

In the presence of a quantizing magnetic field, the Landau levels of the surface subbands, as well as those of the conduction band of PbTe are observed in the tunneling characteristics. Figure 4 shows the d^2I/dV^2-V curves of a junction at several magnetic field intensities. The magnetic field H is applied perpendicular to the plane of the junction at 4.2 °K. Although the structure in the data appears complicated, it is not difficult to recog-

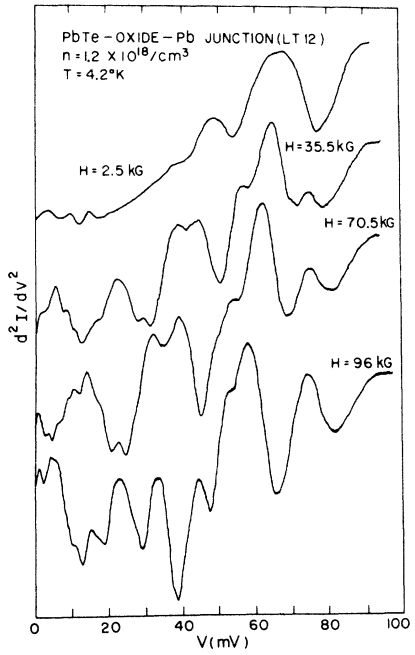

FIG. 4. d^2I/dV^2-V curves of junction LT12 at several magnetic field intensities. The magnetic field is applied perpendicular to the plane of the junction at 4.2°K. A magnetic field, $H \approx 2$ kG, is required to quench the superconductivity of Pb.

nize some of the features, which suggest its having an origin in the Landau levels of the PbTe electrode. First, the magnetic field indeed induces structure in the d^2I/dV^2-V curves. Second, none of this structure is observed for $V > V_0$. In other words, the new structure occurs in the bias range corresponding to the energy levels of electrons in the conduction band and the surface subbands of PbTe. Third, the strength, as well as the bias position, of the structure depends strongly on H. These features are more clearly illustrated in Fig. 5, which shows an alternative way of displaying the Landau level structure in the tunneling characteristics.

In Fig. 5 the d^2I/dV^2 signal is plotted as a function of H when V is kept constant. At a constant V, the Fermi level of the Pb electrode stays at an energy eV away from the Fermi level of PbTe. When H is increased, it changes the energy position of the Landau levels in PbTe, and the d^2I/dV^2-H curve registers a structure whenever a Landau level is moved across the Fermi level of the Pb electrode. If we recall that the Shubnikov–de Haas (SdH) oscillations, in the magnetoresistance of a bulk PbTe sample, register the Landau levels crossing the Fermi level of PbTe, it is obvious that the magnetic-field-induced structure in the d^2I/dV^2-H curves should appear similar to the SdH oscillations. The upper two curves ($V = -10$ mV and $V = 0$) illustrate the magnetotunneling data in the bias range $V \lesssim 0$. In this range, the observed oscillatory behavior is dominated by the long-period oscillations, reflecting the Landau levels in the conduction band of PbTe. The short-period oscillations, complicated by beat patterns, reflect the Landau levels in the subbands. The lower three curves, taken together, illustrate the magneto-oscillatory effects due to electrons in the subbands. For example, at $V = 87$ mV, the Fermi level of the Pb electrode lies below the energy minima of the ground-state subband (i.e., $V > V_0$) and, therefore, the Landau level structure observed in the curves, taken at $V = 47.5$ mV and $V = 60$ mV, are conspicuously absent.

In Fig. 6 we plot the bias position of the dips, observed in the d^2I/dV^2-V curves, as a function of H, which is applied perpendicular to the surface. The data are limited to the bias range in which the magneto-oscillatory effects arise primarily from the electrons in the subbands. For $V \gtrsim V_1$, the data points group themselves into distinct levels, which, if extrapolated to $H = 0$, converge approximately onto the ground-state quantum level at $V = 78$ mV. These levels can, therefore, be assigned to the Landau levels of the ground-state subband. For $V < V_1$, this is not the case and we shall make no attempt to identify the Landau levels which give rise to the observed tunneling structure. We emphasize that the energy associated with the

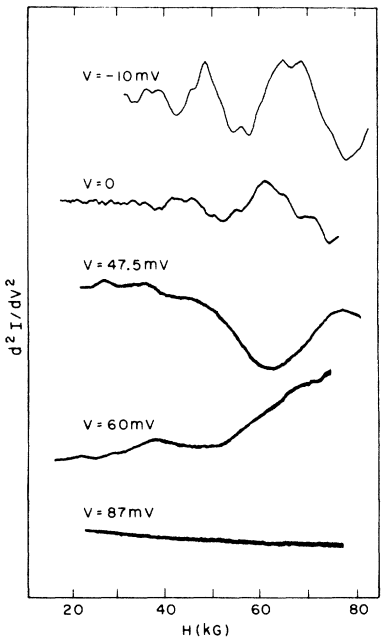

FIG. 5. d^2I/dV^2-H curves at constant V of sample LT12.

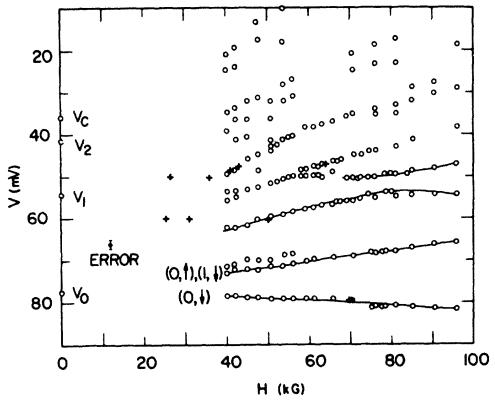

FIG. 6. A summary of data on the Landau level oscillations of the subbands of sample LT12. The circles indicate the dips in the d^2I/dV^2–V curves as a function of H; the crosses indicate the dips in the d^2I/dV^2–H curves as a function of V.

cyclotron frequency of interest here is comparable to the energy separating the two excited states of the quantum levels and also to the energy separating the second excited quantum level from the conduction-band continuum. Consequently, the Landau levels as calculated using Stern and Howard's treatment of a single subband may not represent the actual magnetic energy levels in the excited-state subbands.

The number and the arrow in the brackets in Fig. 6 indicate the Landau quantum number l and the spin direction assigned to the first two levels of the ground-state subbands. The assignment was made by considering the following.

(i) The downward slope of the first (largest bias) level cannot be caused by a Landau level without taking spin into account.

(ii) The first two levels are also resolved when the magnetic field is applied parallel to a [100] direction in the plane of the sample. This is consistent with previous observations that spin splitting is determined by the total magnetic field, not just the normal component. These two results compel us to assign the first two levels to the spin-split $l=0$ levels.

(iii) Since the effective g factor cannot change drastically in the energy range of interest here, we expect spin splitting in the $l=1$ Landau level as well. However, if the spin-down $l=1$ state is assigned to the third level, the Landau level separation will yield a cyclotron effective mass $m^* \approx 0.03m_0$, which is approximately half that expected from the theory of Stern and Howard. Instead, we assign the (1, ↓) state as well as the (0, ↑) state to the second level.

The following two observations may tentatively be regarded as evidence supporting this assignment. First, at lower magnetic fields, the d^2I/dV^2 structure associated with the second level ($V \approx 70$ mV), as seen in the $H=53.5$ kG curve of Fig. 4, has a weak shoulder in the smaller bias side. This shoulder may result from an energy difference between the (1, ↓) and the (0, ↑) states. Second, at higher magnetic fields, when the ratio of level broadening to level separation is small, the d^2I/dV^2 structure loses this shoulder. However, as seen in the $H=96$ kG curve of Fig. 4, the d^2I/dV^2 structure associated with the second level appears considerably stronger than that associated with the first level. This difference in strength is consistent with our energy-level assignment which makes the second level doubly degenerate.

In Fig. 7 we plot the difference in bias of the first two levels of Fig. 6 as a function of H. According to the energy-level assignment discussed in the last paragraph, this difference is given by

$$\nabla V = g^* \mu_B H/e \quad , \tag{8}$$

where μ_B is a Bohr magneton and g^* is the effective g factor of electrons in the ground-state subband. Within the experimental uncertainty, as indicated by the error bars, ΔV varies linearly with H. The slope of a best fit straight line yields $g^* = 29 \pm 3$, which is approximately 18% smaller than its bulk value of 35.5. By using the Landau splitting being equal to the spin splitting, we obtain the effective cyclotron mass for the ground-state subband, $m^* = (0.069 \pm 0.008)m_0$. It differs from the subband cyclotron mass ($0.063m_0$), calculated from the parabolic band model [Eqs. (3) and (5)]. This difference, however, is well within our experimental error. We notice that this mass differs appreciably from the bulk cyclotron mass

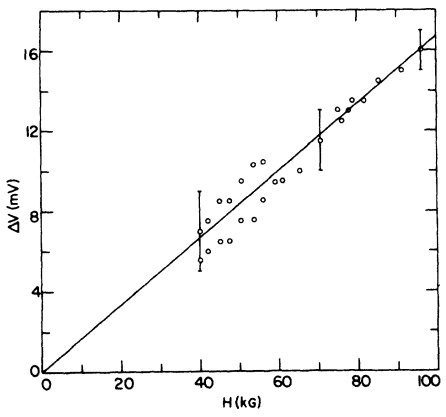

FIG. 7. Magnetic field dependence of ΔV, which is the bias separating the two d^2I/dV^2 dips associated with spin-split $l=0$ Landau levels of the ground-state subband.

$(0.038m_0)$. This large difference, which has been predicted by Stern and Howard, is due to the fact that electrons in the surface subband, unlike those in the bulk, are not allowed to move parallel to the magnetic field.

Antcliffe, Bate, and Reynolds[20] demonstrated, by a quasiclassical calculation, that mass enhancement can also result from the surface quantization of a nonparabolic band. If we recall that the ground-state quantum level is higher in energy than the conduction-band edge in the surface space-charge layer, the quantization may be regarded as causing a widening of the direct band gap of carriers in the surface layer. This increase in energy gap gives rise to an increase in m^* and a decrease in g^*. Qualitatively, our observing a heavier mass and a smaller g factor is in accordance with the fact that the conduction band of PbTe is highly nonparabolic. Any quantitative account of our results must await a quantum-mechanical treatment of the surface space-charge layer, which takes into account the conduction-band nonparabolicity and the spin-orbit coupling.

Enhancement in the mass, as well as the g factor, of electrons in a (100) surface inversion layer on p-Si has previously been reported.[12,21] In both cases, the enhancement appears more pronounced when the surface electron concentration is low ($N_s \lesssim 10^{12}/\text{cm}^2$), and it has, therefore, been attributed to electron-electron interactions.[22] It is clear from the large experimental uncertainties that our experiment cannot detect any many-body effects in either m^* or g factor which is smaller than 10% of its single-particle value. In addition, r_s (the interelectron spacing measured in units of the effective Bohr radius) estimated from the bulk parameters of our samples is ≈ 0.034 and the surface electron concentration is $N_s = 1.9\times10^{13}/\text{cm}^2$. It is, therefore, not surprising that we do not observe any many-body effects in either the electron g factor or its effective mass.

Figure 6 also shows that the Landau levels of the ground-state subband do not intersect the Landau levels of the first-excited-state subband. In the case of a spherical energy-band model, there is no interaction between Landau levels of different subbands and intersection of two Landau levels[3,4] is allowed. However, if the conduction band is nonparabolic or, in the case of an anisotropic parabolic band, the surface normal is not parallel to a principal axis of the constant-energy ellipsoid, interaction between Landau levels in different subbands is expected. The interaction is most important near the crossover of two levels, where even weak coupling can have a large effect. This interaction is most clearly seen in the data at $V \approx 52$ mV and $H \approx 80$ kG in Fig. 6. The splitting at $H = 80$ kG is $\Delta E \approx 4$ meV.

V. SUMMARY

Using tunneling through n-type PbTe-oxide-Pb junctions, we have studied the electronic properties of an accumulation layer at the PbTe-oxide interface. For a sample having $n = 1.2\times10^{18}/\text{cm}^3$, the accumulation layer has a surface electron concentration $N_s = 1.9\times10^{13}/\text{cm}^2$. Three quantum levels, resulting from quantization of the electronic motion normal to the surface, are observed in the Pb (+) bias at $V_0 = 78$ mV, $V_1 = 55$ mV, and $V_2 = 42$ mV. Since the Fermi energy of electrons in the conduction band, determined directly from the tunneling data, is $\mu = 36 \pm 2$ meV, these three levels are at $E_0 = 42$ meV, $E_1 = 19$ meV, and $E_2 = 6$ meV below the conduction-band edge. The depth of the surface potential well is estimated to be $U_0 = 72$ meV.

When a magnetic field is applied perpendicular to the plane of the junction, the tunneling data exhibit magneto-oscillatory effects. We have obtained the following two results from the magneto-oscillatory effect, which reflect the Landau levels in the ground-state subband. First, the ground-state subband has $g^* = 29 \pm 3$ and $m^* = (0.069 \pm 0.008)m_0$. Second, the Landau levels in the ground-state subband do not cross the Landau levels in the excited-state subband. The interaction between the Landau levels removes the degeneracy at the crossover and a splitting, $\Delta E \approx 4$ meV, has been observed.

We have not obtained any direct information on the origin of the accumulation layer. However, it is known that the junction properties of a metal-PbTe contact are determined by the difference between the work function (Φ_m) of the metal and the electron affinity (χ) of PbTe. In the case of Pb ($\Phi_m = 4.0$ eV)[23] on PbTe ($\chi = 4.6$ eV from Ref. 24 and $\chi = 5.1$ eV from Ref. 25), Nill *et al.*[15] have demonstrated that an accumulation layer results on an n-type crystal and an inversion layer results on a p-type crystal. In our case of a PbTe-oxide-Pb tunnel junction, we expect the oxide layer to take up most of the difference between χ and Φ_m. The small value of U_0 deduced from our data is consistent with an explanation that the accumulation layer arises from the mismatch between Φ_m and χ. Unfortunately, we have not been able to fabricate tunnel junctions using other metals as counter-electrode to verify this explanation.

It should also be mentioned that we have not succeeded in fabricating tunnel junctions on either the (110) or the (111) surfaces of PbTe crystals. As for the tunnel junctions on the (100) surface, even the best quality junctions still appear noisier than the InAs-oxide-Pb junctions previously studied.[1] We plan to experiment with various surface cleaning and oxidation methods to overcome these

difficulties. It is also apparent that a determination of the electronic structure in the excited subbands in the presence of an intense magnetic field will require more realistic theoretical guidance as well as better quality junctions. We hope that this paper may stimulate new theoretical interest in this quantum-mechanical problem.

ACKNOWLEDGMENTS

We are grateful to G. A. Baraff and J. M. Rowell for many discussions concerning this work.

[1]D. C. Tsui, Phys. Rev. B 4, 4438 (1971); 8, 2657 (1973); in *Proceedings of the Eleventh International Conference on the Physics of Semiconductors, Warsaw*, 1972 (PWN—Polish Scientific Publishers, Warsaw, 1972), Vol. 1, p. 109.

[2]T. Hagiwara, O. Mizuno, and S. Tanaka, J. Phys. Soc. Jap. 34, 973 (1973).

[3]C. B. Duke, Phys. Rev. 159, 632 (1967); D. J. Ben-Daniel and C. B. Duke, Phys. Rev. 160, 679 (1967); C. B. Duke, Phys. Lett. A 24, 461 (1967).

[4]G. A. Baraff and J. A. Appelbaum, Phys. Rev. B 5, 475 (1972).

[5]J. N. Zemel and M. Kaplit, Surf. Sci. 13, 17 (1969).

[6]F. Stern and W. E. Howard, Phys. Rev. 163, 816 (1967).

[7]I. Giaever and K. Megerle, Phys. Rev. 122, 1101 (1961).

[8]W. L. McMillan and J. M. Rowell in *Superconductivity*, edited by R. D. Parks (Marcel Dekker, New York, 1969), Chap. 11.

[9]Yu. I. Ravich, B. A. Efimova, and I. A. Smirnov, *Semiconducting Lead Chalcogenides* (Plenum, New York, 1970), Chap. 6.

[10]C. K. N. Patel and R. E. Slusher, Phys. Rev. 177, 1200 (1969).

[11]C. Kittel, *Quantum Theory of Solids* (Wiley, New York, 1963), p. 203.

[12]F. F. Fang and P. J. Stiles, Phys. Rev. 174, 823 (1968).

[13]J. M. Rowell, W. L. McMillan, and W. L. Feldmann, Phys. Rev. 180, 658 (1969).

[14]R. N. Hall and J. H. Racette, J. Appl. Phys. 32, 2078 (1961).

[15]K. W. Nill, J. N. Walpole, A. R. Calawa, and T. C. Hartman, in *The Physics of Semimetals and Narrow Gap Semiconductors*, edited by D. L. Carter and R. T. Bate (Pergamon, New York, 1971), p. 383.

[16]D. C. Tsui, Solid State Commun. 9, 1789 (1971).

[17]L. Y. L. Shen, J. Appl. Phys. 40, 5171 (1969); G. I. Rochlin and P. K. Hansma, Phys. Rev. B 2, 1460 (1970).

[18]J. Zavadil, Phys. Lett. A 43, 437 (1973).

[19]See, for example, D. Colman, R. T. Bate, and J. P. Mize, J. Appl. Phys. 39, 1923 (1968).

[20]G. A. Antcliffe, R. T. Bate, and R. A. Reynolds, in Ref. 15, p. 499.

[21]J. L. Smith and P. J. Stiles, Phys. Rev. Lett. 29, 102 (1972); A. A. Lakhani and P. J. Stiles, Phys. Rev. Lett. 31, 25 (1973).

[22]J. F. Janak, Phys. Rev. 178, 1416 (1969); T. Ando, Y. Matsumoto, and Y. Uemura in *Proc. of the Eleventh International Conference on the Physics of Semiconductors, Warsaw*, 1972 (PWN—Polish Scientific Publishers, Warsaw, 1972), Vol. 1, p. 294.

[23]J. C. Riviere in *Solid State Surface Science*, edited by M. Green (Marcel Dekker, New York, 1969), p. 245.

[24]W. E. Spicer and G. T. Lapyre, Phys. Rev. 139, A565 (1965).

[25]M. Green, M. J. Lee, and R. E. Miles, Surf. Sci. 12, 403 (1968).